PHYSICAL REVIEW B
CONDENSED MATTER

THIRD SERIES, VOLUME 29, NUMBER 4 15 FEBRUARY 1984

New look at the line shape of differential reflectograms for dilute alloys

R. E. Hummel
Department of Materials Science and Engineering, University of Florida, Gainesville, Florida 32611

R. Enderlein
Alexander von Humboldt Universität zu Berlin, DDR-108 Berlin, German Democratic Republic
(Received 11 April 1983; revised manuscript received 14 November 1983)

A complete line-shape analysis of experimental differential reflectograms of dilute alloys is presented. Two different types of transitions near the L-symmetry point are considered for transitions in the near-infrared, visible, and near-ultraviolet spectrum. The energies for interband transitions as well as the lifetime-broadening energy are obtained directly from the experimental differential reflectograms without using an unmodulated reflectivity spectrum and a Kramers-Kronig analysis. Transition energies obtained from an experimental differential reflectogram for a Cu—1.5 at. % Ga alloy are given.

I. INTRODUCTION

Differential reflectometry has proven valuable in investigating details about the electron structure around the Fermi surface of metals and alloys.[1] This technique has been shown to provide, within one-hundredth of an electron volt, the energies which electrons absorb from photons as they are raised into higher, allowed states. The technique involves the periodic and small variation of the solute content within a binary-alloy system ("compositional modulation").

Enderlein *et al.*[2] have developed a line-shape analysis for differential reflectograms for the fundamental absorption edge which reproduced remarkably well the experimental spectra of copper-based alloys. From this line-shape analysis, the threshold energy for interband transitions and the lifetime-broadening parameter were obtained.

Other investigators[3,4] used modulated reflectivity data in conjunction with static reflectivity data and deduced from them $\Delta\epsilon_2$, using Kramers-Kronig analyses (ϵ_2 is the imaginary part of the complex dielectric constant). The latter analysis requires the extrapolation of R and $\Delta R/R$ beyond the experimental range. This procedure does not cause substantial error if one can assume that no structure exists beyond the measured spectral range, an assumption which is probably valid only in rare occasions. Rosei *et al.*[5–7] calculated separately the imaginary part of the dielectric constant for copper and for the alloys. Then they convoluted them with different "broadening parameters" and subsequently obtained $\Delta\epsilon_2$ spectra by numerical subtraction.

This paper presents a rigorous approach to the analysis of the line shape of differential reflectograms which includes all the observed peaks in compositional modulation spectra in the near ir, visible, and near uv for α-copper-based alloys. The transition energies and the lifetime-broadening parameter are obtained *directly* from the experimental differential reflectograms without the aid of a Kramers-Kronig analysis and static reflectivity data.

II. CALCULATION OF LINE SHAPE

It is suggested that two different types of transitions near the L-symmetry point are mainly responsible for the structures seen in compositional modulation spectra (in the near ir, visible, and near uv) of α-copper-based alloys: transitions from d bands well below the Fermi level into the free-electron-like L_2' band just above the Fermi level [Fig. 1(a)], transitions from the same L_2' band into the L_1 band well above the Fermi level [Fig. 1(b)]. The initial band will be referred to as band 1, and the final one as band 2. The change ΔX of alloy composition X affects both types of transitions for the same reasons: Firstly, because of a shift of energy bands; secondly, because of the change of lifetime broadening; and thirdly, because of a shift of the Fermi level with respect to the bottom of the L_2' band. All three changes are taken into account in our calculation. Other effects, such as changes of transition matrix elements or changes of effective masses are as-

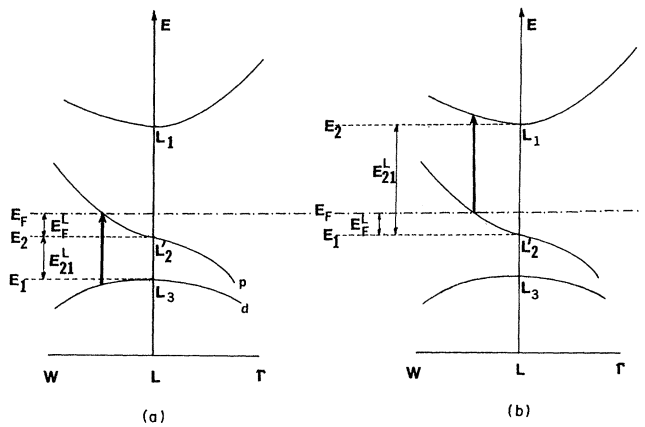

FIG. 1. Band model for optical transitions around the L-symmetry point; (a) transitions *to* the Fermi level, and (b) transitions *from* the Fermi level.

sumed to be small. The result of the effects mentioned is a change of the complex dielectric function $\Delta\epsilon=(d\epsilon/dX)\Delta X$, which can be related to the relative change $\Delta R/R$ of reflectance by means of the equation

$$\frac{\Delta R}{R}=\left[\alpha\frac{d\epsilon_1}{dX}+\beta\frac{d\epsilon_2}{dX}\right]\Delta X\ , \tag{1}$$

where α and β are the Seraphin coefficients[8] and ϵ_1 and ϵ_2 are the real and imaginary parts of ϵ, respectively. In the spectral region of interband transitions, ϵ can be calculated from the expression

$$\epsilon=-\frac{4\pi e^2}{\hbar\omega^2 m^2}\int\frac{d^3k\,|p_{21}(\vec{k})|^2}{4\pi^3}\times\frac{f(E_1(\vec{k}))-f(E_2(\vec{k}))}{\hbar\omega-[E_2(\vec{k})-E_1(\vec{k})]+i\hbar\Gamma}\ , \tag{2}$$

where E_1 and E_2 are the energies of the initial and the final bands, respectively, $\hbar\Gamma$ is the lifetime-broadening energy of the interband excitation, p_{21} is the transition matrix element, and f is the Fermi distribution function.

Let us consider at first the model of isotropic parabolic bands using

$$E_i(k)=E_i^L+\frac{\hbar^2}{2m_i}k^2\quad(i=1,2) \tag{3a}$$

and

$$p_{21}(\vec{k})=\text{const}\ . \tag{3b}$$

This model does not reproduce completely the transition in compositional modulation spectra. Actually the transitions terminate or start at the L_2' band in the vicinity of the Fermi level at which the band structure is far from being isotropic. The present case, however, provides some qualitative insights which aid in the understanding of the actual case which we will treat below.

We commence with transitions *to* the Fermi level [Fig. 1(a)]. In this case the initial band $E_1(\vec{k})$ is completely occupied, i.e., $f(E_1(\vec{k}))=1$. The final band $E_2(\vec{k})$ is occupied below the Fermi level, i.e., $f(E_2(\vec{k}))=1$ for $\hbar^2k^2/2m_2<E_F^L$ and empty above the Fermi level, i.e., $f(E_2(\vec{k}))=0$ for $\hbar^2k^2/2m_2>E_F^L$. Transforming the $\vec{k}$ integral in (2) into an integral upon the kinetic energy $E=\hbar^2k^2/2m_2$ of band 2, ϵ becomes (disregarding a constant factor)

$$\epsilon\sim-\int_{E_F^L}^{\infty}dE\frac{\sqrt{E}}{\hbar\omega-E_{21}^L-(m_2/m_{21})E+i\hbar\Gamma}\ , \tag{4}$$

where E_{21}^L means the energy separation between bands 2 and 1 at L, and m_{21} is the corresponding reduced effective mass (we assume $m_{21}>0$). The derivative of ϵ from Eq. (4) with respect to the alloy composition X consists of two terms, one term denoted by $(d\epsilon/dX)_F$ for the derivative with respect to the Fermi energy E_F^L at the lower integral boundary in (4) and one term denoted by $(d\epsilon/dX)_T$ for the derivative of the denominator of the integral in (4) with respect to $-E_{21}^L$. One obtains

$$\frac{d\epsilon}{dX}=\left[\frac{d\epsilon}{dX}\right]_F+\left[\frac{d\epsilon}{dX}\right]_T\ , \tag{5}$$

$$\left[\frac{d\epsilon}{dX}\right]_F\sim\frac{dE_F^L}{dX}\frac{1}{\omega-\omega_T+i\Gamma}\ , \tag{6}$$

$$\left[\frac{d\epsilon}{dX}\right]_T\sim\left[\frac{m_{21}}{m_2}\right]\left[\frac{dE_{21}^L}{dX}-i\hbar\frac{d\Gamma}{dX}\right]\left[\frac{1}{\omega-\omega_T+i\Gamma}-\frac{1}{2}\frac{1}{[\omega_0(\omega-\omega_T+i\Gamma)]^{1/2}}\ln\frac{(\omega_0)^{1/2}+(\omega-\omega_T+i\Gamma)^{1/2}}{(\omega_0)^{1/2}-(\omega-\omega_T+i\Gamma)^{1/2}}\right]\ , \tag{7}$$

$$\omega_T=\hbar^{-1}\left[E_{21}^L+\frac{m_2}{m_{21}}E_F^L\right],\quad\omega_0=\frac{m_2}{m_{21}}\hbar^{-1}E_F^L\ . \tag{8}$$

The two terms for $(d\epsilon/dX)_T$ in the large parentheses of Eq. (7) were obtained by partial integration. The first term shows the same ω dependence as $(d\epsilon/dX)_F$, whereas the second one does not. The second term, however, is small compared to the first one in the spectral region around $\omega=\omega_T$ where the line-shape structure of interest is located. In other words, as long as

$$\left|\frac{\omega-\omega_T+i\Gamma}{\omega_0}\right|\ll1 \tag{9}$$

is fulfilled, the second term can be neglected. With this

approximation, the line shape of $(d\epsilon/dX)$ becomes very simple,

$$\left[\frac{d\epsilon}{dX}\right]\sim\left[\frac{d\omega_T}{dX}-i\frac{d\Gamma}{dX}\right]\frac{1}{\omega-\omega_T+i\Gamma}\ . \tag{10}$$

If we assume m_1 (the mass of the initial d band) to be infinity, and further assume $d\Gamma/dX=0$, then Eq. (10) provides the same result as was obtained in our earlier paper[2] [see Eq. (11) in Ref. 2].

So far we have considered transitions *to* the Fermi level. In the case of transitions *from* the Fermi level [Fig. 1(b)] we consider $f(E_2(\vec{k}))=0$. Further, $f(E_1(\vec{k}))=1$ for $\hbar^2k^2/2m_1<E_F^L$, and $f(E_1(\vec{k}))=0$ for $\hbar^2k^2/2m_1>E_F^L$. Instead of Eq. (4) one obtains

$$\epsilon\sim-\int_0^{E_F^L}dE\frac{\sqrt{E}}{\hbar\omega-E_{21}^L-(m_1/m_{21})E+i\hbar\Gamma}\ . \tag{11}$$

With the use of the same arguments as before, relation (11) yields approximately

$$\left[\frac{d\epsilon}{dX}\right]\sim-\left[\frac{d\omega_T}{dX}-i\frac{d\Gamma}{dX}\right]\frac{1}{\omega-\omega_T+i\Gamma}\ , \tag{12}$$

$$\hbar\omega_T=\left[E_{21}^L+\frac{m_1}{m_{21}}E_F^L\right]\ . \tag{13}$$

As expected, the line shape of $d\epsilon/dX$ remains the same as in the former case. Only the definition of ω_T is slightly altered, and an additional minus sign occurs in (12) which accounts for the fact that the transition energy is lowered if the Fermi energy (or the band crossing it) goes up.

Let us consider now the actual case that is an anisotropic band L_2'. Parabolicity is assumed as before. It will be shown that the same expressions (10) and (12) can be applied for $d\epsilon/dX$ as in the isotropic case. We stipulated above that the spectral structure of $d\epsilon/dX$ may be attributed to transitions near L. Thus the $\vec{k}$ integral in the general expression for $d\epsilon/dX$ [differentiating Eq. (2) with respect to X] can be restricted to a certain volume V and L. The transition matrix element $p_{21}(\vec{k})$ will be assumed to be constant in V. First we consider transitions *to* the Fermi surface. For the execution of the $\vec{k}$ integral upon V, new variables $[E_2(\vec{k}), u(\vec{k}),$ and $v(\vec{k})]$ are introduced. Here, u and v are the surface coordinates of the surface $E_2(\vec{k})=$const. Let $D(E_2,u,v)$ be the Jacobian of this transformation. The integral upon E_2 can be readily taken for the derivative $(d\epsilon/dX)_F$. The remaining surface integral upon the part FS(V) of the Fermi surface within volume V is approximated by replacing the transition energy in the denominator by the average value

$$\hbar\omega_T=E_F^L+E_{21}^L+\frac{\int_{\mathrm{FS}(V)}dS\,D}{\int_{\mathrm{FS}(V)}dS\,D[E_1^L-E_1(E_F^L,u,v)]^{-1}}\ . \tag{14}$$

From that we obtain

$$\int_{\mathrm{FS}(V)}dS\frac{D}{\hbar\omega-[E_2^L-E_F^L-E_1(E_F^L,u,v)]}=\frac{\int_{\mathrm{FS}(V)}dS\,D}{\hbar\omega-\hbar\omega_T+i\hbar\Gamma}\ . \tag{15}$$

Thus $(d\epsilon/dX)_F$ takes the same form as in (6). The derivative $(d\epsilon/dX)_T$ can be separated into two terms such as in the isotropic case, one term being proportional to (15) and one term being small compared to it in the vicinity of $\omega=\omega_T$. Thus the total derivative of ϵ with respect to X takes the form (10) which is also true in the case of nonisotropic parabolic bands. Only the definition of $\hbar\omega_T$ has to be taken from (14) instead of (13). The same arguments apply to transitions *from* the Fermi level. In this case expression (12) holds also for $d\epsilon/dX$ for nonisotropic parabolic bands. Both types of transitions can be combined into one simple line-shape expression for $(\Delta R/R)$. Equation (1) can then be written as

$$\left[\frac{\Delta R}{R}\right]=\mathrm{Re}\left[(\alpha-i\beta)\frac{d\epsilon}{dX}\right]\ . \tag{16}$$

With $d\epsilon/dX$ from (10) and (12) one obtains

$$\left[\frac{\Delta R}{R}\right]\sim\mathrm{Re}\left[(\alpha-i\beta)\left[\frac{d\omega_T}{dX}-i\frac{d\Gamma}{dX}\right]\frac{1}{\omega-\omega_T+i\Gamma}\right]\ . \tag{17}$$

Introducing the complex numbers

$$Ce^{i\rho}=\alpha-i\beta\ , \tag{18}$$

$$\left[\frac{d\omega_T}{dX}-i\frac{d\Gamma}{dX}\right]=\left[\left[\frac{d\omega_T}{dX}\right]^2+\left[\frac{d\Gamma}{dX}\right]^2\right]^{1/2}e^{i\Psi}\ ,$$

and setting $\rho+\psi=\theta$, Eq. (17) assumes the final form

$$\frac{\Delta R}{R}=A\left[\left[\frac{d\omega_T}{dX}\right]^2+\left[\frac{d\Gamma}{dX}\right]^2\right]^{1/2}F\left[\frac{\omega-\omega_T}{\Gamma},\theta\right]\ , \tag{19}$$

$$F(s,\theta)=\sin\phi(s)\cos[\phi(s)-\theta]\ , \tag{20}$$

$$\phi(s)=\arcsin\frac{1}{(1+s^2)^{1/2}}\ , \tag{21}$$

where A is a factor which is independent of X and depends only slightly on ω. The line-shape curves $F(\omega-\omega_T/\Gamma,\theta)$ have been plotted in Ref. 2 for various values of θ and are reproduced in Fig. 2. By fitting our experimental $\Delta R/R$ spectrum (Fig. 3) to the calculated line-shape equation (19) the transition energy $E_T=\hbar\omega_T$ and the broadening energy $\hbar\Gamma$ can be obtained as a function of X. The shift of the transition energy E_T results from two contributions, that is, the shift of the Fermi level E_F^L and the change of the band separation with respect to X.

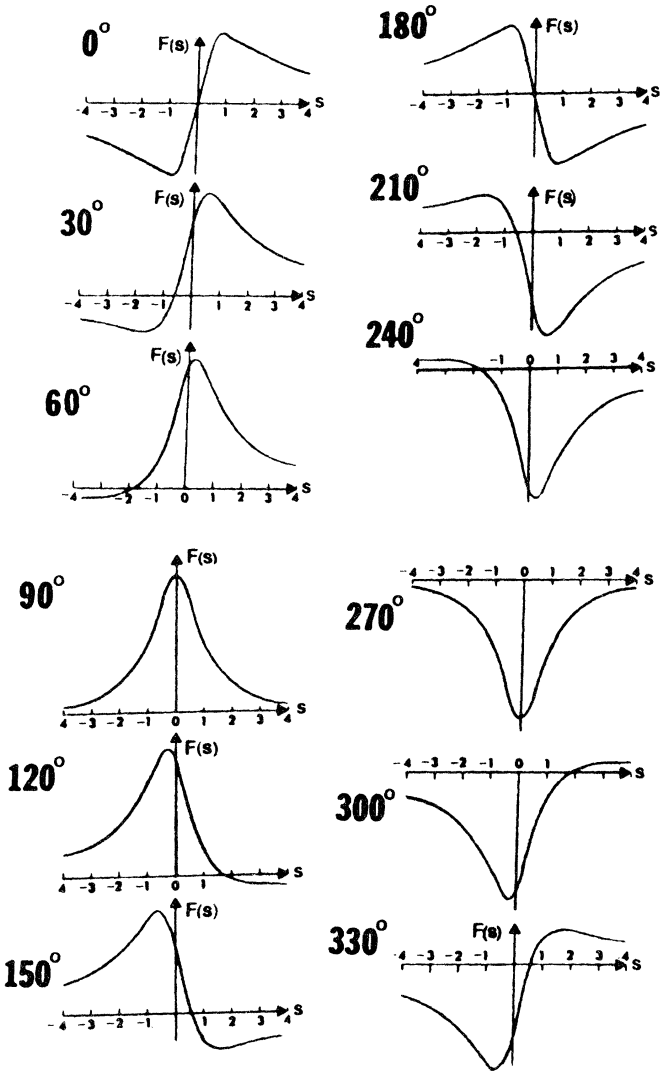

FIG. 2. $F(s,\theta)$ vs s for selected θ values (from Ref. 2).

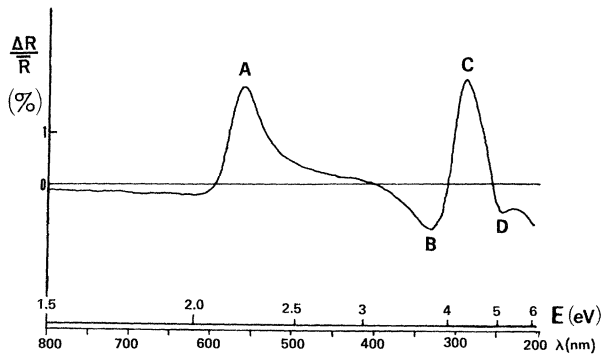

FIG. 3. Experimental differential reflectrogram ($\Delta R/\bar{R}$ vs photon energy E) for a Cu—1.5 at.% Ga alloy (average alloy composition: The two specimens consisted of a Cu—1 at.% Ga and a Cu—2 at.% Ga alloy, respectively).

III. DISCUSSION

Carotenuto *et al.*[6] reanalyzed some of our compositional modulation spectra[9] taken on dilute Cu-Al and Cu-Zn alloys. They utilized their line-shape analysis mentioned in the Introduction and concluded that even at low solute concentrations the absorption edge of the L_3-L_2' (E_F) transition moves toward higher energies with respect to its position in pure copper. This is in contrast to our findings which indicate that the threshold energy for interband transitions, E_T, does not vary appreciably for solute concentrations up to slightly above 1 at.%.[10] Our findings confirm the prediction by Friedel[11] who postulated screening effects of the solute valence electrons at low solute concentrations. Carotenuto *et al.* argue that a peak in $\Delta R/\bar{R}$ can only be explained if one assumes a shift of the transition energy (E_T) to higher energies with increasing X. A shift of E_T is, however, not necessary for a peak in $\Delta R/\bar{R}$. Equation (17) shows that a $\Delta R/\bar{R}$ signal is obtained even for $d\omega_T/dX=0$ because of lifetime-broadening effects (i.e., $d\Gamma/dX\neq 0$). This becomes particularly evident in differential reflectograms for copper-gold[1,10] and copper-nickel[1,12] alloys in which a broadening of the threshold peak with high solute concentration can be clearly seen. It is believed that the data reduction used by Carotenuto *et al.*[6] (Kramers-Kronig analysis, etc.) may have simulated the shift in $E_T=f(X)$ for small solute concentrations.

A further point seems to be significant. Both transitions considered here, namely that *to* the Fermi energy and that *from* the Fermi energy lead to a line shape which has the same features [see Eqs. (10) and (12)]. Only the value of θ is different. For example, for peak A (in Fig. 3), θ is approximately 60° and E_T is close to the maximum.[2] On the other hand, for features B and C in Fig. 3, θ may be assumed to be close to 0°, which leads to a transition energy somewhere between minimum B and maximum C. Experimental observations suggest that features B and C are indeed part of *one* transition: When the energies of peaks B and C are plotted versus the solute concentration, both curves are essentially parallel to each other.[12] The inflection points in the curves of Fig. 2 can be used for the characterization of θ.

Finally, feature D in Fig. 3 behaves in many respects similarly to peak A (increase in E_T with increasing X) and has therefore been assigned in the past to transition from the *lower d* bands to the Fermi energy. The inversion of peak D with respect to peak A stems from the negative α/β ratio in the former case.[1]

The line shape of the differential reflectogram shown in Fig. 3 (Cu—1.5 at.% Ga) has been analyzed with the method put forward in this paper. The following results have been obtained for peak A: $\theta^A=61°$; threshold energy $E_T^A=2.19$ eV; lifetime-broadening energy $\hbar\Gamma^A=1.6\times10^{-2}$ eV. For the double peak B,C, one obtains $\theta^{BC}=0°$ and $E_T^{BC}=4.02$ eV. Finally, for peak D we obtain $\theta^D\approx 330°$ and $E_T^D=5.1$ eV.

IV. CONCLUSION

The complete line shape of differential reflectograms obtained in the near ir, visible, and near uv spectra for dilute copper-based alloys can be reproduced by assuming transitions around the L-symmetry point and applying a non-isotropic but parabolic band model. We further conclude that compositional modulation is a first-derivative technique, and that the energies for interband transitions and the lifetime broadening can be calculated.

[1]R. E. Hummel, Phys. Status Solidi A 76, 11 (1983), and papers quoted herein.
[2]R. Enderlein, R. E. Hummel, J. B. Andrews, R. J. Nastasi-Andrews, and C. W. Shanley, Phys. Status Solidi B 88, 173 (1978).
[3]R. E. Prange, H. D. Drew, and J. B. Ristorff, J. Phys. C 10, 5083 (1977).
[4]D. Beaglehole and E. Erlbach, Phys. Rev. B 6, 1209 (1972).
[5]R. Rosei, S. Modesti, V. Prantera, and I. Davoli, J. Phys. F 9, 2275 (1979).
[6]C. Carotenuto, R. Rosei, and M. Sommacal, Solid State Commun. 19, 547 (1976).
[7]A. Balzarotti, E. Colavita, S. Gentile, and R. Rosei, Appl. Opt. 14, 2412 (1975).
[8]B. O. Seraphin and N. Bottka, Phys. Rev. 145, 628 (1966).
[9]R. E. Hummel and J. B. Andrews, Phys. Rev. B 8, 2449 (1973).
[10]R. J. Natasi-Andrews and R. E. Hummel, Phys. Rev. B 16, 4314 (1977).
[11]J. Friedel, Proc. Phys. Soc. London Sect. B 65, 769 (1952).
[12]R. E. Hummel, J. Alfaro Holbrook, and J. B. Andrews, Surf. Sci. 37, 717 (1973).